Airflow Optimization for Room Air Conditioners

Tanaka, Ryuta; Nabi, Saleh; Nonaka, Mio

Abstract

The purpose of this paper is to increase the energy eff

ciency of room air conditioners (RAC) while achieving a comfortable indoor space. We pose the problem as a multi-objective optimization problem in which the design variables are the inlet temperature, air speed, and angle. The multi-objective function constitutes of the temperature uniformity of the room and average wind in the room in a region of interest as representative of thermal comfort, and a function of coefficient of performance (COP) as representative of the energy consumption of the RAC. Direct-adjoint-looping (DAL) method is used as the method for optimization, which is a gradient-based method. We also compared and analyzed the effects of various models of RACs on energy savings and comfort.

Building Simulation 2021 Conference

Airflow optimization for Room air conditioners

Ryuta Tanaka[1], Saleh Nabi[2], Mio Nonaka[1]
[1]MITSUBISHI ELECTRIC Corporation, Amagasaki, Japan
[2]Mitsubishi Electric Research Laboratories, Cambridge, USA

Abstract

The purpose of this paper is to increase the energy efficiency of room air conditioners (RAC) while achieving a comfortable indoor space. We pose the problem as a multi-objective optimization problem in which the design variables are the inlet temperature, air speed, and angle. The multi-objective function constitutes of the temperature uniformity of the room and average airflow velocity in the room in a region of interest as representative of thermal comfort, and a function of coefficient of performance (COP) as representative of the energy consumption of the RAC. Direct-adjoint-looping (DAL) method is used as the method for optimization, which is a gradient-based method. We also compared and analyzed the effects of various models of RACs on energy savings and comfort.

Key Innovations

- Implemented adjoint-based optimization for the task of both thermal comfort maximizing and minimizing the energy consumption within the built environment.

- Developed a multi-physics framework, which incorporates the impact of refrigerant cycle dynamics into the dynamics of the turbulent air flow within the built environment.

- Compared and assessed the impact of various design variables to control the thermal comfort and energy consumption by increasing the degrees of freedom.

- Compared and assessed the impact of each term in the multi-objective cost function, namely thermal comfort versus the energy consumption.

Practical Implications

Adjoint-based analysis has several advantages over conventional trial-and-error computational fluid dynamics (CFD) of achieving optimal conditions in the room. The practical importance of the work is twofold: i) it provides a systematic method, with mathematical guarantees, to seek optimal design variables to maximize thermal comfort within the room while decreasing the energy consumption. ii) our method highlights the importance of using sophisticated control strategies and degrees of freedom in the design of next generation HVAC equipment.

Introduction

Modern buildings are a major contributor to energy consumption in North America, largely due to the Heating, Ventilation and Air Conditioning (HVAC) requirements (Cipra (2013)). It is also evident that indoor airflow greatly affects occupant comfort, health, and productivity. In the past few decades, the field of architectural fluid dynamics has seen considerable advances in the form of better theoretical understanding of buoyancy-driven indoor flows, novel experimental techniques, and advanced numerical methods (Chen (2009)). There is a rising interest in combining such recent advances with modern optimization and control methods for the purpose of optimal design and control of flow in the built environment (Nabi et al. (2019); Bewley (2001)). This engineering task has the twin goals of maintaining thermal comfort while reducing energy consumption. The complicated dynamics of airflow within the built environment, and its interaction with occupants, building, and the exterior, necessitate a systematic approach to accomplish this task.

There are various methods to determine air velocity, temperature, relative humidity, and contaminant concentration in a room, such as computational fluid dynamics (CFD), analytical models, and experimental measurements. However, such methods most often employ a trial-and-error process to design HVAC systems that achieve desired conditions in the built environment (Liu and Chen (2015)). This process can become computationally intractable for large number of design variables, rely on domain expertise, and does not come with a mathematical guarantee for the optimality.

Recently, many researchers have attempted to use optimization methods such machine-learning (ML) based methods (Mousa et al. (2017)), genetic algorithm (GA) method (Xue et al. (2013)) and reduced order modeling (Vijayshankar et al. (2020)), which come with many promises. However, such methods still are very expensive in terms of training the models and lack appropriate physical interpretation.

The *adjoint method* has long been identified as the method of choice for optimization in fluid mechanics (Anderson and Venkatakrishnan (1999); Othmer (2008)). Indoor airflow optimization is aimed at obtaining optimal boundary actuation (either steady or

time-varying) that leads to desired airflow temperature and velocity distribution characteristics in the domain of interest. In the past decade, application of systematic optimization and control to indoor airflow has been gaining attention (Liu and Chen (2015)). A parallel but related recent development is the use of nonlinear adjoint optimization techniques to find 'optimal', i.e. minimal energy, perturbations that lead to turbulence in canonical flows.

In our previous work (Nabi et al. (2017)), we formulated and solved a model test-case problem of *optimal design* to determine *steady* inlet velocity and temperature that optimize a certain cost functional related to achieving a desired temperature distribution in part of a room using the Direct-Adjoint-Looping (DAL) method (Nabi et al. (2017, 2019)). That study focused on the fully turbulent mixed-convection regime, resulting from the presence of a line heat source in addition to forced conditioned air from the inlet. Since DNS/LES based numerical optimization is not feasible with reasonable computing resources, we employed Reynolds-Averaged Navier-Stokes (RANS) models to account for interaction between the mean-flow and turbulent eddies. We validated the numerically computed optimal solutions with those obtained by optimizing experimentally-verified analytical reduced-order models for the same problem.

In this paper, we extend our previous work by extending the results of 2D case studies, to 3D case studies. We also consider the important impact of airflow velocity on the thermal comfort of occupants and investigate how the relative importance of temperature to velocity component of thermal comfort can alter the optimal solution within the room. Finally, we take into account the energy consumption of the refrigerant cycle associated with RAC with analytical models. The rest of the paper is organized as follows. In Section 2, we discuss the model and describe the schematic of the problem. We also formulate the optimal control problem and discuss the implementation of the DAL method to solve such problems. In Section 3, we discuss the results of the optimal design problem, and the dependence of optimization results on various problem parameters. In Section 4, we provide conclusions and sketch out directions for future research.

Methods

Problem Setup

The optimization problem setup is planned to optimize the airflow of a typical indoor RAC. The room size is designed based on the typical room size where RACs are installed in homes. In the heating mode, the temperature stratification is more pronounced than the cooling mode, which can lead to thermal discomfort. Therefore, we focus on the heating mode, for which the walls are at lower than thermal comfort
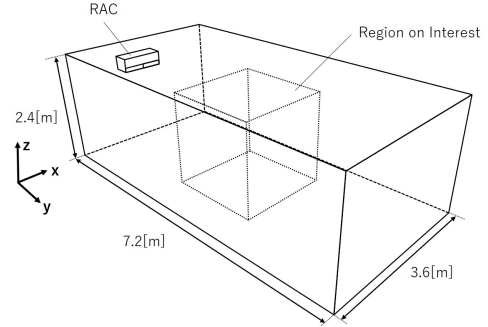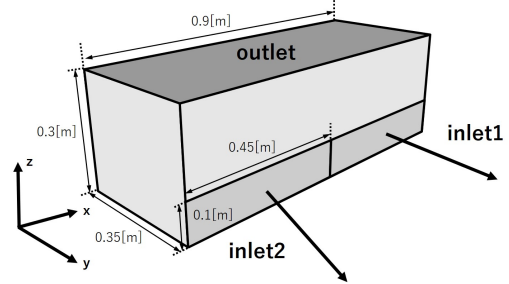

Figure 1: lab model.

Figure 2: rac model.

level temperature, as a more challenging case. Furthermore, there is a need to reduce power consumption from the perspective of energy efficiency. The COP curve in this paper is defined as a function of the load factor under typical heating conditions. Using such definition of COP, the problem of minimizing the energy consumption of RACs can be solved in a consistent way in the same framework as that of the thermal comfort. In the control problem of RAC, the size of the fan or compressor performance has constraints on the inlet temperature and airflow speed. By keeping the design variables within these constraints, the optimal solution realized in this optimization can be realistically reproduced in the RAC in a room or a laboratory.

Figure 1 shows the size of the laboratory model. The fresh and conditioned air is supplied into the room via the RAC in Fig. 2, served as the inlet boundary condition, at a left x-z wall in vicinity of the ceiling. In this study, we consider two types of RACs. The first design involves only one inlet and therefore the design variables are inlet velocity and temperature i.e. $\mathbf{V}_{in}, T_{in}$. The inlet velocity vector design variables are, in particular, the normal velocity V_{in}^y, which determines the volume flux supplied to the room, the yaw angle θ_{xy}, and the pitch angle θ_{zy} defined below

$$\theta_{xy} = arctan\left(\frac{V_{in}^x}{V_{in}^y}\right) \quad (1)$$

$$\theta_{zy} = arctan\left(\frac{V_{in}^z}{V_{in}^y}\right) \quad (2)$$

The second design, which is the main focus of this study, considers two inlets, each has its own normal

Table 1: Thermal boundary conditions for the walls

North	South	East	West	Ceiling	Floor
24.5°C	24°C	24°C	24°C	25°C	20°C

velocity, pitch, and yaw angles denoted by $V_{in,i}^y$, $\theta_{xy,i}$, and $\theta_{zy,i}$, with $i \in 1, 2$ represents the number of inlet. It is assumed, however, both inlets share the same temperature T_{in}. Typical Reynolds number in our experiments are $7500 < Re < 15000$.

The air is exhausted through an outlet located right above the RAC. In this study, we considered an empty room and the impact of heat sources are modeled as the iso-thermal walls. The details of each wall thermal boundary condition is shown in Table 1, which are evaluated using experimental data in our prototype lab. Due to the asymmetry in wall temperatures, there will be vertical and horizontal temperature disparities leading to an adverse impact on the thermal comfort of the occupants. Moreover, the velocity of air supply may has a negative impact on the thermal comfort. In the meantime, thermal comfort in the room should be maintained with minimal energy consumption. Therefore, the task of optimization is to identify the optimal air supply inlet conditions, i.e. volume flux, angles, and temperature, that improve the overall thermal comfort level in the occupant region while minimizing the energy consumption.

Governing Equations

The turbulent flow is governed by Boussinesq equations described below (using Einstein notation)

$$\frac{\partial v_j}{\partial x_j} = 0,$$
$$\frac{\partial v_i v_j}{\partial x_j} + \frac{\partial p_i}{\partial x_i} - g\beta\delta_{i3}(T - T_{ref}) - \frac{\partial}{\partial x_j}(\nu_{eff}\frac{\partial v_i}{\partial x_j}) = 0,$$
$$\frac{\partial v_j \theta}{\partial x_j} - \frac{\partial}{\partial x_j}(\kappa_{eff}\frac{\partial T}{\partial x_j}) = 0,$$

$$(3)$$

with $\mathbf{v}, p, T$ as ensemble-averaged velocity, pressure and temperature, the vertical direction is the third coordinate direction, and δ_{ij} is the Kronecker delta. We use $T_{ref} = T_{comf}$. g and β are gravitational acceleration and coefficient of expansion, respectively. ν_{eff} and κ_{eff} are effective viscosity and diffusivity. We assume $Pr = 0.71$ as the Prandtl number of air at room temperature. Boundary conditions are as follows:

$$\text{inlet}: \mathbf{v} = \mathbf{V}_{in}, T = T_{in}, (n_i \partial/\partial x_i)p = 0,$$
$$\text{outlet}: (n_i \partial/\partial x_i)v_i = 0, (n_i \partial/\partial x_i)T = 0, p = 0, \quad (4)$$
$$\text{wall}: \mathbf{v} = 0, T = T_{wall}, (n_i \partial/\partial x_i)p = 0,$$

where $\mathbf{n}$ is the unit vector normal to the surface. The velocity and temperature at inlet are denoted by $\mathbf{V}_{in}$

and T_{in}, respectively.

Cost Function and Adjoint Equations

In this section, we formally describe the optimization problem. The region of interest, denoted by Ω, is a cubical region shown in Fig. 1 to mimic a typical occupant region in a typical room. T_{comf} and $\mathbf{v}_{comf}$ denote the desired velocity and temperature to be maintained in Ω. We set $\mathbf{v}_{comf} = \mathbf{0}$ and $T_{comf} = 26.5°C$; however, it should be noted that the analysis is independent of the specific T_{comf} value. We define the cost function as

$$\mathcal{J} = \int_{\Omega} \left[\gamma_T(T(x,y,z) - T_{comf})^2 + \right. $$
$$\left. \gamma_v (\mathbf{v}(x,y,z) - \mathbf{v}_{comf})^2 \right] dV$$

$$(5)$$

where γ_T, γ_v as weighting factors. Hence, the thermal comfort model considered in this paper constitutes of a temperature component, first term of Eq. 5 and a airflow or velocity component, i.e. the second term of Eq. 5. The ratio of $\frac{\gamma_T}{\gamma_v}$ determines the relative importance of each term, which is studied in this paper. The optimization problem for such a cost function is formulayted as

$$\min_{\mathbf{V}_{in}, T_{in}} \mathcal{J} = \mathcal{J}(\mathcal{W}, \mathcal{U}),$$
$$\text{s.t. } \mathcal{R}(\mathcal{W}, \mathcal{U}) = 0,$$

$$(6)$$

where $\mathcal{W} = (\mathbf{v}, p, T)$ are the state variables, namely, velocity vector, pressure and temperature, and $\mathcal{U}$ is the set of design variables, i.e., $\mathcal{U} = (\mathbf{V}_{in}, T_{in})$. $\mathcal{R}$ denotes the constraints arising from the state governing equations, corresponding to the Boussinesq equations 3. Additional constraints may also be implemented with no change in the formulation of Eq. (6).

We tackle the optimization problem by using the notion of the Lagrangian $\mathcal{L}$ to enforce the Boussinesq equations and constraints, as

$$\min_{\mathbf{V}_{in}, T_{in}} \mathcal{L} = \mathcal{J} + <\mathcal{P}, \mathcal{R}>, \quad (7)$$

where $\mathcal{P} = (\mathbf{v}_a, p_a, T_a)$ is the vector of adjoint variables, and we use the notation $\langle f, g \rangle = \int_{\mathbb{D}} fg \, dV$ with $\mathbb{D}$ as the whole domain. The adjoint variables are Lagrange multipliers to enforce the state equations Eq. (3). To ensure the (at least local) optimality of the solution, we enforce $\delta\mathcal{L} = \delta_{\mathcal{U}}\mathcal{L} + \delta_{\mathcal{W}}\mathcal{L} = 0$, where δG denotes variation of a dependent variable G. We choose the adjoint variables such that $\delta_{\mathcal{W}}\mathcal{L} = 0$. The sensitivity equations with respect to control variables are then obtained as $\delta\mathcal{L} = \delta_{\mathcal{U}}\mathcal{L}$. This idea is the core of the adjoint method- see e.g. Othmer (2008); Nabi et al. (2017).

By enforcing that first order variations with respect to the state variables vanish at optimal solutions, i.e.,

$\delta_{\mathcal{W}}\mathcal{L} = 0$, we obtain the adjoint equations

$$\frac{\partial v_{a,j}}{\partial x_j} = 0,$$

$$v_{a,j}\frac{\partial v_j}{\partial x_i} - v_j\frac{\partial v_{a,i}}{\partial x_j} + T_a\frac{\partial T}{\partial x_i} - \frac{\partial}{\partial x_j}(\nu_{eff}\frac{\partial v_{a,i}}{\partial x_j})$$

$$+ \frac{\partial p_a}{\partial x_i} = -\gamma_v v_i,$$

$$- g\beta\delta_{i3}v_{a,i} - v_j\frac{\partial T_a}{\partial x_j} - \frac{\partial}{\partial x_j}(\kappa_{eff}\frac{\partial T_a}{\partial x_j}) = -\gamma_T(T - T_{comf})$$

$$(8)$$

The adjoint boundary conditions are

$$\text{inlet}: \mathbf{v}_a = 0, T_a = 0, (n_i\partial/\partial x_i)p_a = 0,$$
$$\text{outlet}: p_a.\mathbf{n} = (\mathbf{v}_a.\mathbf{n})\mathbf{v}_a + \nu_{eff}(n_i\partial/\partial x_i)\mathbf{v}_a,$$
$$T_a(\mathbf{v}_a.\mathbf{n}) + \kappa_{eff}(n_i\partial/\partial x_i)T_a = 0,$$
$$\text{wall}: \mathbf{v}_a = 0, (n_i\partial/\partial x_i)T_a = 0, (n_i\partial/\partial x_i)p_a = 0,$$

$$(9)$$

We use the 'frozen turbulence' hypothesis (Papoutsis-Kiachagias and Giannakoglou (2016)) in deriving Eq. 8. As a result of this assumption, the effective viscosity used in Eq. 8 is obtained from the $k - \epsilon$ equations solved along with the direct system of equations Eq. 3. An assessment of the validity of this assumption has been carried out in Nabi et al. (2017).

The gradient of the cost function with respect to inlet velocity and temperature is obtained as follows.

$$\nabla_{V_{in}}\mathcal{J} = p_{a,in} - \nu_{eff}(n_i\partial/\partial x_i)v_{a,in},$$
$$\nabla_{T_{in}}\mathcal{J} = \kappa_{eff}(n_i\partial/\partial x_i)T_{a,in},$$

$$(10)$$

In order to update the inlet conditions, we apply a gradient descent method of the form:

$$T_{in}^{k+1} = T_{in}^k - \frac{\partial \mathcal{J}}{\partial T_{in}}^k,$$

$$(11)$$

where superscript k denotes the number of iteration. Similar equation can be written for the inlet velocity. We illustrate the iterative solution procedure schematically in Fig. 3, which shows the algorithm for the DAL method. The optimization begins with an initial guess for the design variables $\mathbf{V}_{in}, T_{in}$. The set of 'direct' or forward equations and adjoint equations are solved in a loop and the subsequent sensitivity calculation is used to obtain the next guess for the optimal design variables. This process is repeated until the convergence criterion for the cost functional is satisfied. For a complete details on derivation, verification, and validation of DAL please see our previous works Nabi et al. (2017, 2019).

Details of Numerical Solver

We use the finite-volume solver OpenFOAM. This solver uses a collocated grid arrangement and offers
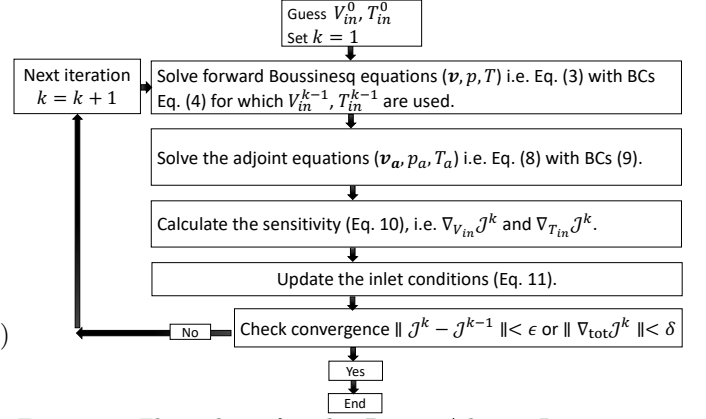

Figure 3: Flow chart for the Direct-Adjoint-Looping (DAL) method.

object-oriented implementations that suit the employed continuous adjoint formulation. Pressure and velocity are decoupled using the SIMPLE algorithm of Patankar and Spalding (1972) in the direct/adjoint equations. For the convection terms, second order Gaussian integration is used with the Sweby limiter (Sweby (1984)) for numerical stability. For diffusion, Gaussian integration with central-differencing-interpolation is used. The discretized algebraic equations are solved using the Preconditioned biconjugate gradient (PBiCG) method (Ferziger et al. (1997)). The adjoint equations are also solved using the numerical method described for solving the forward or direct equations. We found that using an upwind and first order method for solving the adjoint equations Eqs. 8 resulted in inaccurate gradients, and hence those methods were not adopted.

Model for refrigerant cycle performance and energy consumption

As shown in Fig. 2, the RAC model has two inlets and one outlet. To determine the energy consumption of RAC, we calculate the heat load based on the inlet and outlet temperature and volume flux as follows

$$x = \frac{1}{W_{ref}}\int_{\Gamma_{inlet}}\bar{V}_{in}(T_{in} - T_{out})dS$$
$$COP = ax^3 + bx^2 + cx + d$$
$$COP_x = 3ax^2 + 2bx + c$$
$$J_{pow} = \frac{x \cdot W_{ref}}{COP},$$

$$(12)$$

where the coefficients $a, b, c,$ and d were determined based on experimental data. $\bar{V}_{in}$ is the average inlet velocity across the two inlets. J_{pow} is representative of energy consumption by the RAC for a given set of heat load and inlet boundary conditions. As shown in Eq. 12, the closed-form of COP as a function of heat load ratio x, enables us to analytically calculate the gradient of cost function with respect to the inlet

conditions, using chain rule

$$\frac{dJ_{pow}}{dT_{in}} = \frac{dJ_{pow}}{dx}\frac{dx}{dT_{in}},$$
$$\frac{dJ_{pow}}{dV_{in}} = \frac{dJ_{pow}}{dx}\frac{dx}{dV_{in}} \tag{13}$$

Analytical form of $\frac{dJ_{pow}}{dT_{in}}$ and $\frac{dJ_{pow}}{dV_{in}}$ can be calculated in a straightforward fashion. We then modify out total cost function as

$$\mathcal{J} = \int_{\Omega}\left[\gamma_T(T(x,y,z) - T_{comf})^2 + \right.$$
$$\left. \gamma_v\big(\mathbf{v}(x,y,z) - \mathbf{v}_{comf}\big)^2\right]dV + wJ_{pow} \tag{14}$$

We refer to the first two terms, i.e. Eq. 5 as J_{comf}. To calculate the sensitivity we sum up Eq. 10 and $w\times$ Eq. 13. We should mention that two types of RAC are considered in this study: type I, for which inlet 1 and 2 are assumed to be unified and hence only 1 inlet is considered (4 design variables in total consisting of three components of velocity and temperature) and type II, for which inlets 1 and 2 are independent in terms of velocity but share the same temperature (7 design variables in total consisting of 2 sets of three components of velocity and temperature). Finally, for a realistic simulation and optimization, we enforced box constraints on the minimum and maximum of the inlet velocity and temperature.

Results and Discussion

To verify the performance of the DAL method with consideration of thermal comfort, minimal airflow, and energy consumption of the refrigerant cycle in the presence of kinematic and dynamic constraints of the RAC for optimal design of an indoor environment, we conducted a series of case studies for representative lab described in previous sections.

The direct and adjoint simulation time for a typical case, consisting of 518,070 finite volumes, is, respectively 1764 sec, and 1326 sec on a compute node with 10 CPUs each with the clock speed of 3.458 GHz. Thus, the total simulation time of one DAL cycle is 3090 sec. Mesh study is applied for the number of mesh points and the quantity of interest, i.e. cost function of Eq. 5 becomes almost independent of the number of finite volumes in the current mesh (Richardson extrapolation of Shyy et al. (2002)). Several iterations may be required for DAL to converge depending on the initial guess. The convergence criteria for the DAL optimization were that $\|J^k - J^{k-1}\| < \epsilon$ or the overall gradient is $\nabla_{tot}J^k < \delta$, where $k \geq 2$ is the iteration of each DAL cycle, $\epsilon = 1e - 3$, and $\delta = 1e - 4$). The overall gradient $\nabla_{tot}J$ is defined as the root mean square of all gradients.

Table 2 summarizes all cases considered in this study. All cases are at steady-state. Three important com-

parison are to be made: the comparison of cases 2 and 3 to illustrate the impact of RAC type, i.e., having one versus two inlets), the comparison of cases 1 and 2 to demonstrate the impact of γ_V/γ_T, i.e., the influence of temperature versus velocity in the thermal comfort model, the comparison of cases 1, 4, and 5 to clarify the impact of w, i.e., power consumption, respectively, on the optimal results.

We begin our analysis by discussing common features for all optimization case studies. As illustrated in Fig. 4, the cost function reduces gradually with successive DAL cycle for all cases. Moreover, as depicted in Fig. 5, the overall gradient decreases with each iteration, which is expected, as the optimization iterations follow the opposite of the gradient, the cost function approaches to the local minima, which corresponds to a smaller gradient values. To avoid inclusion of all gradients, we only focus on the overall gradient as well as gradient with respect to $x-$component of velocity, i.e. $\nabla_{V_{in}^x}J$ for reasons become clear below.

The first case for which a more detailed analysis is provided, is the optimization of the supply velocity and temperature for type II RAC with $\gamma_v = 1$, $\gamma_T = 1$. For the first round of optimization, we neglect the energy consumption and focus only on the thermal comfort. As shown in Table 2, the yaw angle θ_{xy} for the optimal solution is almost 0, implying the jet of incoming flow is towards the center of the room with very slight deviation. This is due to the symmetrical thermal boundary conditions in the lateral walls. The optimal solution at steady-state is shown in Fig. 6-a. As shown, the strong jet of relatively warmer air is descending into the room, upon which, entrainment of the ambient air towards the jet is occurred, resulting in strong mixing between the RAC airflow and that of the room. Therefore, an ambient with characteristics of a well-mixed room is developed. Since, the temperature component of thermal comfort is dominant in this case, such well-mixedness is ensued with strong airflow in Ω. The reduction of cost function and the overall gradient for this case are also shown in Fig. 4(a) and 5(a), respectively.

To study the impact of the the design variables on the nature of thermal comfort, we also study the optimization of design variables of RAC of design II where $\gamma_v = 1$ and $\gamma_T = 0.001$ (dubbed as case 2 in Table 2), such that the temperature and airflow components of the thermal comfort have almost the same order. As shown in Table 2, the design variables for such alternative cost function are non-trivially different. Of particular interest is the yaw angle which is towards left and right of the room for inlet 1 and 2, respectively, as opposed to the center injection of the optimal solution for case 1. This is due to the fact that there is a meaningful emphasize on reducing airflow in the region of interest. Such results are reaffirmed by looking into optimal values of θ_{xy} in

Table 2: Various case studies for optimization of thermal comfort and energy consumption for two types of RAC.

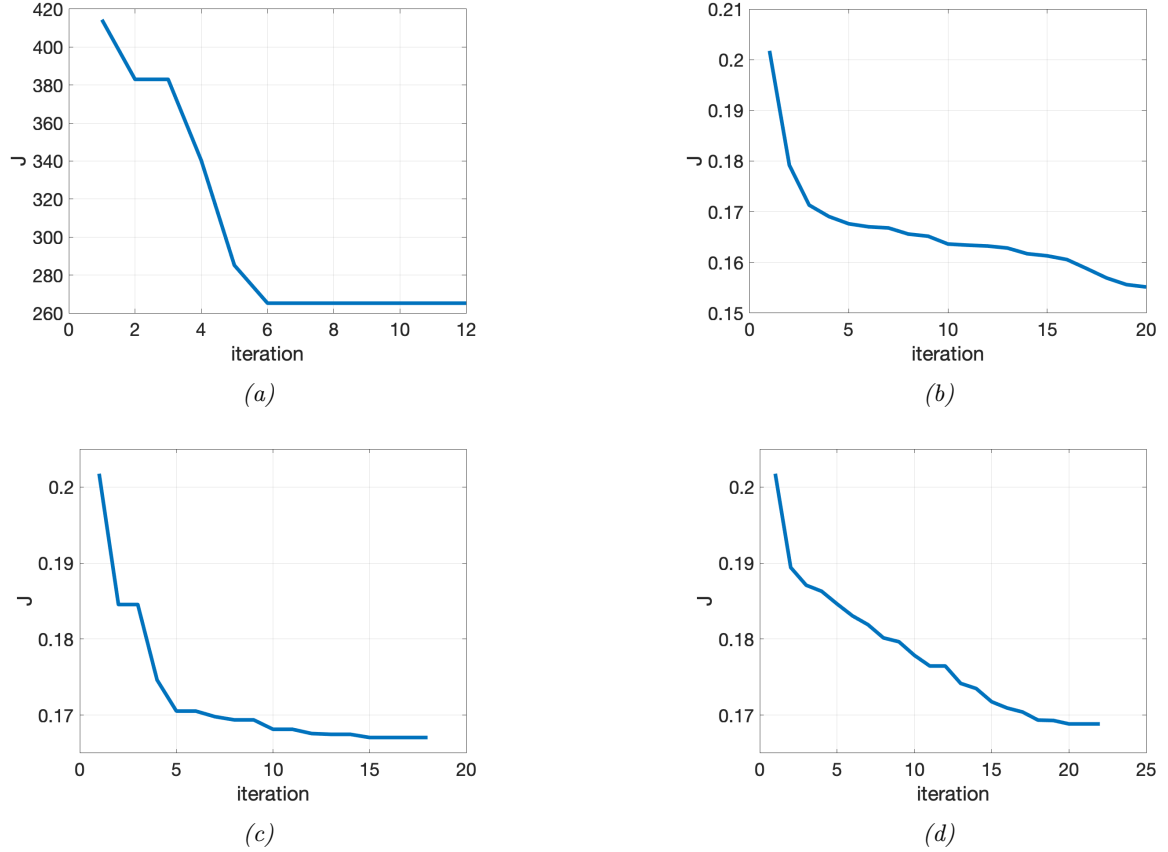| Case No.	RAC type	γ_v, γ_T, w	$V_{in,1}^y, \theta_{xy,1}, \theta_{xz,1}, T_{in}$ optimal values	$V_{in,2}^y, \theta_{xy,2}, \theta_{xz,2}$ optimal values
1	II	$1, 1, 0$	$2.51, -0.13°, 50°, 34.5°C$	$2.37, 0.12°, 37°$
2	II	$1, 0.001, 0$	$1.87, -26°, 23°, 44.3°C$	$1.67, 22°, 29°$
3	I	$1, 0.001, 0$	$1.62, -35.6°, 50°, 42.4°C$	N/A
4	II	$1, 0.001, 0.1$	$1.63, -32°, 50°, 41.6°C$	$1.66, 35°, 50°$
5	II	$1, 0.001, 1$	$1.64, -32°, 50°, 40.0°C$	$1.66, 36°, 51°$

Figure 4: Objective function with respect to number of DAL cycles, denoted as iterations for (a) case 1, (b) case 2, (c) case 3, and (d) case 4.

Table 2, which is approximately less than 1° for case 1, while it is $|\theta_{xy}| \approx 26°$ for case 2. As shown in Fig. 5, such values of θ_{xy} in each case result in very small values of $\nabla^x_{V_{in}} J$ at the end of iterations. Comparison of case 2 and 3 reveals the importance of the cost function on the design variables and indicates different physical processes are favored based on such a choice. The optimal solution of case 2 is shown in Fig. 6-b.

As the third case, we consider the optimization of the supply velocity and temperature for a type I RAC, i.e. one inlet types, with $\gamma_v = 1$ and $\gamma_T = 0.001$. The optimal solution of case 3 is shown in Fig. 6-c. As indicated, the airflow component is slightly larger in vicinity of RAC with some differences in the temperature distribution in the room. With reference to Fig.

4, we observe that the optimal cost function related to type II has a lower value, and hence more optimized solution, compared to type I. Results of comparison of case 2 and 3 demonstrate that i) DAL is successful to increase the thermal comfort of occupants, while satisfying the constraints, systematically for all designs, and ii) design II, i.e. RAC with two separate inlets, due to having higher degrees of freedom for the design variables, is able achieve 8% smaller cost function, which proves more sophisticated designs are more favorable in terms of thermal comfort of the occupants in the built environment.

As an important part of this study, we consider cases 4 and 5, which are type II designs with $\gamma_v = 1$ and $\gamma_T = 0.001$ but with inclusion of energy consumption. For case 4 and 5 the weight for energy consumption
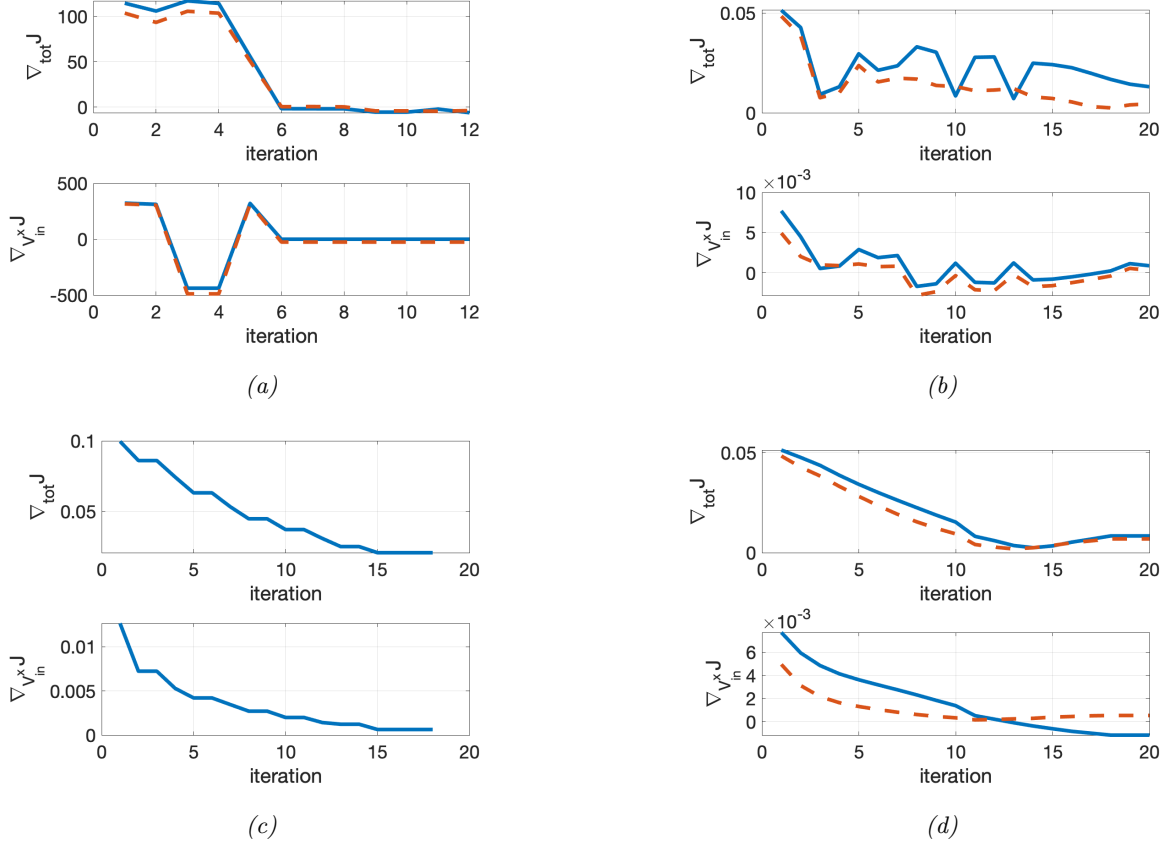
Figure 5: Overall gradient, $\nabla_{tot}J$, as top panel and gradient with respect to the $x-$component of velocity, $\nabla_{V_{in}^x} J$, as a function of DAL iterations for (a) case 1, (b) case 2, (c) case 3, and (d) case 4. For type II RAC, the blue/solid and red/dotted curves denote, respectively, sensitivity with respect to inlet 1 and inlet 2.

is $w = 0.1$ and 1, respectively. For case 4, J_{pow} has a similar order of magnitude as J_{comf} while for case 5, the energy consumption is relatively more important. The streamlines of case 4 are not very different than that of case 2 and hence not included. Also, as is evident in Table 2, the optimal solution of case 5 and 4 are very similar, which signifies that for moderate values of weighting for energy consumption, the optimal solution is relatively robust and does not alter significantly with w. Due to the similarities of cases 4 and 5, only results for case 4 are included in Figs. 4 and 5. It should be noted that for very large values of w, the minimum allowable velocity is the optimal solution, since thermal comfort becomes negligible. Finally, during the optimization process using DAL, 16% reduction in overall cost, i.e. $J_{comf} + J_{pow}$ from the initial guess, is osberved in case 4.

Conclusion

In this paper, we studied the problem of optimizing the temperature and velocity distribution in a domain containing turbulent buoyancy-driven flow associated with a RAC injected in a room. The method for the optimization is adjoint-based sensitivity analysis, which we proved as a DAL algorithm. We validated such problems in the past for 2D flows with no consid-

eration of energy consumption. An important contribution of this paper is to consider a realistic 3D turbulent flow with box constraints for design variables by taking into account the energy consumption.

We studied the impact of i) cost function choice, e.g. relative weightings of temperature to velocity components in J_{comf}, ii) degrees of freedom, e.g. type I and type II RACs, and iii) energy consumption by considering $w = 0, 0.1$, and 1 for steady-state on the optimal design variables. Our results demonstrate that depending on the choice of thermal comfort model, a higher airflow with almost well-mixed room, or a lower airflow with larger stratification can be the optimal velocity and temperature distribution. Implementing a correct thermal comfort model requires consideration of several other parameters such as air relative humidity, clothing, and even mindset of occupants, which in turn necessitates consideration of additional constraints that is beyond the scope of the present manuscript. Nonetheless, our proposed framework is able to accommodate more complicated cost functions.
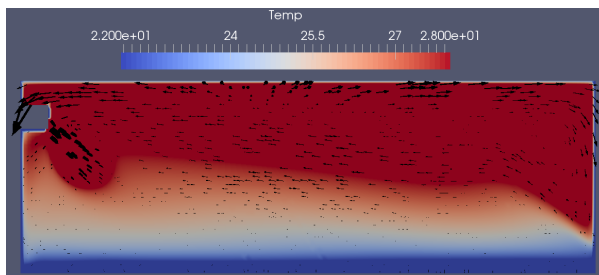
Our knowledge about the physics of the problem considered in this study assists us to start with a guess that does not result in numerical problems. Hence,
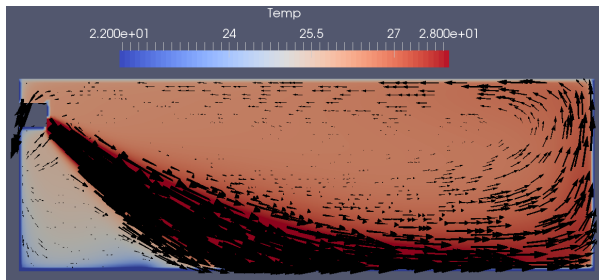
(a)
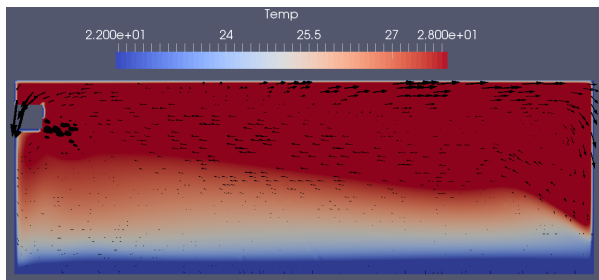
(b)

(c)

Figure 6: Streamlines, in black, superposed on a colormap of the temperature for the optimal solution corresponding to case 1-3. Results are shown in the midcenter plane.

the reduction in the cost functions observed in Fig. 4 are of important value as they start with an intelligent guess. DAL, similar to other gradient-based optimization methods, is seeking local minima. In this study, we used multistart initial guess strategy to ensure the quality of optimization.

Next steps include, validation of the optimization results using similitude experiments.

References

Anderson, W. K. and V. Venkatakrishnan (1999). Aerodynamic design optimization on unstructured grids with a continuous adjoint formulation. *Computers & Fluids 28*(4), 443–480.

Bewley, T. R. (2001). Flow control: new challenges for a new renaissance. *Progress in Aerospace sciences 37*(1), 21–58.

Chen, Q. (2009). Ventilation performance prediction for buildings: A method overview and recent applications. *Building and environment 44*(4), 848–858.

Cipra, B. A. (2013). Energy-efficient building design. [Online; accessed 20-February-2017].

Ferziger, J. H., M. Peric, and A. Leonard (1997). Computational methods for fluid dynamics.

Liu, W. and Q. Chen (2015). Optimal air distribution design in enclosed spaces using an adjoint method. *Inverse Problems in Science and Engineering 23*(5), 760–779.

Mousa, W. A. Y., W. Lang, T. Auer, and W. A. Yousef (2017). A pattern recognition approach for modeling the air change rates in naturally ventilated buildings from limited steady-state cfd simulations. *Energy and Buildings 155*, 54–65.

Nabi, S., P. Grover, and C. Caulfield (2019). Nonlinear optimal control strategies for buoyancy-driven flows in the built environment. *Computers & Fluids 194*, 104313.

Nabi, S., P. Grover, and C.-c. P. Caulfield (2017). Adjoint-based optimization of displacement ventilation flow. *Building and Environment 124*, 342–356.

Othmer, C. (2008). A continuous adjoint formulation for the computation of topological and surface sensitivities of ducted flows. *International Journal for Numerical Methods in Fluids 58*(8), 861–877.

Papoutsis-Kiachagias, E. and K. Giannakoglou (2016). Continuous adjoint methods for turbulent flows, applied to shape and topology optimization: industrial applications. *Archives of Computational Methods in Engineering 23*(2), 255–299.

Patankar, S. V. and D. B. Spalding (1972). A calculation procedure for heat, mass and momentum transfer in three-dimensional parabolic flows. *International journal of heat and mass transfer 15*(10), 1787–1806.

Shyy, W., M. Garbey, A. Appukuttan, and J. Wu (2002). Evaluation of richardson extrapolation in computational fluid dynamics. *Numerical Heat Transfer: Part B: Fundamentals 41*(2), 139–164.

Sweby, P. K. (1984). High resolution schemes using flux limiters for hyperbolic conservation laws. *SIAM journal on numerical analysis 21*(5), 995–1011.

Vijayshankar, S., S. Nabi, A. Chakrabarty, P. Grover, and M. Benosman (2020). Dynamic mode decomposition and robust estimation: Case study of a 2d turbulent boussinesq flow. In *2020 American Control Conference (ACC)*, pp. 2351–2356. IEEE.

Xue, Y., Z. J. Zhai, and Q. Chen (2013). Inverse prediction and optimization of flow control conditions for confined spaces using a cfd-based genetic algorithm. *Building and Environment 64*, 77–84.